Multiplicities of forward-backward particles in ^{16}O-emulsion interactions at 4.5 AGeV/c *

LI Hui-Ling(李惠玲) ZHANG Dong-Hai(张东海)[1)] LI Jun-Sheng(李俊生)

(Institute of Modern Physics, Shanxi Normal University, Linfen 041004, China)

Abstract An exclusive study of the characteristics of interactions accompanied by backward emission ($\theta_{\rm lab} \geqslant 90^\circ$) of shower and grey particles in collisions of a 4.5 AGeV/c ^{16}O beam with emulsion nuclei is carried out. The experimental multiplicity distributions of different particles emitted in the forward ($\theta_{\rm lab} < 90^\circ$) and backward hemispheres due to the interactions with the two emulsion components (CNO, AgBr) are presented and analyzed. The correlations between the different emitted particles are also investigated. The results indicate that there are signatures for a collective mechanism, which plays a role in the production of particles in the backward hemisphere. Hence, the backward multiplicity distribution of the emitted shower and grey particles at 4.5 AGeV/c incident momentum can be represented by a decay exponential law formula independent of the projectile size. The exponent of the power was found to increase with decreasing target size. The experimental data favor the idea that the backward particles were emitted due to the decay of the system in the latter stages of the reactions.

Key words relativistic heavy-ion collisions, multifragment emission and correlations, nuclear emulsion

PACS 25.75.-q, 25.70.Pq, 29.40.Rg

1 Introduction

Over the last few years, the production of backward particles in hadron-nucleus and nucleus-nucleus interactions at relativistic energies has received considerable experimental and theoretical attention[1—14]. A principal reason for studying the production of energetic pions from nuclei in the backward direction is that, in free nucleon-nucleon collisions such production is kinematically restricted. Therefore, the observation of such hadrons beyond the kinematic limit may then be evidence for exotic production mechanisms such as production from clusters[1—6]. In early experiments[3] at the Dubna Laboratory using incident protons, the authors observed pions in the backward direction with energies up to four times larger than expected from nucleon-nucleon collisions. They argued that the simple Fermi motion of the nucleons in the nucleus could not account for such backward production and stated that the dominant mechanism for producing such hadrons was the interaction between the incident nucleon and multi-nucleon clusters in the target, referring to this mechanism as cumulative production. Fredriksson[15] supported the model in which the nucleon interacts collectively with all matter within 1 fm in its rest frame at the time of collision. The LBL data[2, 8] supported a model called the "effective target model"[4].

In this paper, we analyze the data on shower and grey particles produced in the backward ($90^\circ \leqslant \theta \leqslant 180^\circ$, where θ is the emission angle in the laboratory system) hemisphere and forward ($0^\circ \leqslant \theta \leqslant 90^\circ$) hemisphere from the interaction of ^{16}O projectile with emulsion nuclei at 4.5 AGeV/c. This research focused on the general characteristics of multiplicity distributions of backward shower and grey particles and compared them systematically with the corresponding ones obtained for other projectiles at nearly the same incident momentum per nucleon[16—25]. Furthermore, the multiplicity correlations between dif-

Received 13 October 2008

* Supported by National Natural Science Foundation of China (10475054, 10675077), Natural Science Foundation of Shanxi Province China (200811005) and Shanxi Provincial Foundation for Returned Scholars of China (20031046)

1) E-mail: zhangdh@dns.sxnu.edu.cn

ferent particles were also investigated.

2 Experimental details

NIKFI BR-2 stacks of nuclear emulsions, 10 cm × 10 cm × 2 cm in volume, were exposed horizontally to the 4.5 AGeV/c ^{16}O beam at the Synchrophasotron of the JINR, Dubna. The flux intensity was 10^3 particles/cm^2. Emulsion plates, 600 μm thick were scanned by the along-the-track method using XSJ-1 and XSJ-2 microscopes under 100× oil objectives and 16× eyepieces. Details about scanning, measurements and track classification have been given elsewhere[26—29]. A total of 2960 interactions of oxygen with the nuclei of the emulsion were observed by following a primary track length of 35768.9 cm, which led to a mean free path $\lambda = (12.08 \pm 0.22)$ cm. Among these interactions, 152 events were found to be produced by electromagnetic interactions and 149 events were due to elastic interactions. Of these 2960 interactions, 2044 inelastic interactions were chosen, without any bias, for the final analysis. Interactions which were within 30 μm from the top or bottom surface of the emulsion were not taken into consideration for the final analysis.

Tracks resulting from each event were classified according to the following traditional emulsion terminology.

(1) Shower tracks are single charged relativistic particles with relative ionization $I/I_0 < 1.4$ where I_0 is the plateau ionization for single charged minimum ionizing particles. They are mainly due to produced charged pions having relative velocity $\beta = v/c \geqslant 0.7$. Their multiplicity is denoted by $n_{\rm s}$ (not including the stripped projectile protons).

(2) Grey tracks are those tracks which have a range $R > 3$ mm in emulsion and relative ionization $I/I_0 > 1.4$. They are mostly due to protons with kinetic energy ranging from 26 to 400 MeV. The multiplicity of these grey tracks is denoted by $N_{\rm g}$.

(3) Black tracks are those having short range in emulsion $R \leqslant 3$ mm (corresponding to the proton kinetic energy < 26 MeV). Their multiplicity is denoted by $N_{\rm b}$. Grey and black tracks together are usually considered as heavily ionizing particles. Their multiplicity is denoted by $N_{\rm h} = N_{\rm g} + N_{\rm b}$.

(4) Any charged particle emitted with an angle $\theta \leqslant 3^\circ$, with respect to the incident direction and characterized by no change in its ionization for at least 2 cm from the interaction point, is considered as a noninteracting (stripped) projectile fragment (PF). The total charge of the stripped fragments in the forward cone per event is denoted by Q.

In each event, the total charge of the PFs $Q = \Sigma N_i Z_i$ was calculated, where N_i is the number of the PFs with charge $Z_i (1, 2, \cdots, Z_{\rm p})$ and the summation is carried out over all such fragments in an event. The number of interacting projectile nucleons in each event $N_{\rm int} = A_{\rm p} - (A_{\rm p}/Z_{\rm p})Q$ was determined, where $A_{\rm p}$ and $Z_{\rm p}$ are the mass and charge numbers of the projectile nucleus.

The number $N_{\rm h}$ emitted in an interaction is an important parameter and greatly helps in separating events due to target types, i.e., all events due to H interactions have $N_{\rm h} = 0, 1$. Interactions having $N_{\rm h} \geqslant 8$ almost definitely belong to AgBr collisions, while events with $2 \leqslant N_{\rm h} \leqslant 7$ are due to interactions with CNO and peripheral AgBr. It was found that events due to H, CNO and AgBr were estimated to be 345(16.9%), 776(38.0%) and 923(45.5%), respectively.

3 Experimental results

As already mentioned, hadrons produced in nucleus-nucleus interactions at high energy may originate from two mechanisms. They may participate only in the primary reaction and leave the overlap region of projectile and target without further interaction. In emulsion experiments such hadrons are seen as shower tracks. Or they may be involved in the rescattering process by knocking out further nucleons while penetrating through the spectator parts of the nuclei. The intranuclear cascade is responsible for knocking out cascade protons and neutrons of the spectator fragments. Most of the cascade protons have energies typical for the so-called grey tracks.

The average multiplicities of shower and grey particles emitted in the forward ($\langle n_{\rm s}^{\rm F} \rangle$ and $\langle N_{\rm g}^{\rm F} \rangle$) and the backward ($\langle n_{\rm s}^{\rm B} \rangle$ and $\langle N_{\rm g}^{\rm B} \rangle$) hemispheres for 4.5 AGeV/c ^{16}O interactions are listed in Table 1. For comparison the data from other nuclear interactions with emulsion at nearly the same incident energies (Dubna energies) are also presented. The data in this table show a significant increase in the values of $\langle n_{\rm s}^{\rm B} \rangle$ as the number of incident projectile increases up to ^{7}Li. The values of $\langle n_{\rm s}^{\rm B} \rangle$ within experimental error are nearly equal in the interactions induced by ^{7}Li, ^{12}C, ^{16}O, ^{22}Ne, ^{28}Si and ^{32}S nuclei. On the other hand, the values of the average multiplicity of shower particles produced in the forward hemisphere $\langle n_{\rm s}^{\rm F} \rangle$ are strongly dependent on projectile size (i.e. dependent on the average number of interacting projectile nucleons, $N_{\rm int}$). As the projectile

size increases, a greater number of projectile nucleons interact with the target nucleons. The dependence of $\langle n_s^F \rangle$ on the projectile mass number can be described by the power law relation $\langle n_s^F \rangle = a_s^F A_p^{b_s^F}$ where $a_s^F = 1.726 \pm 0.007$ and $b_s^F = 0.573 \pm 0.002$ (as shown in Fig. 1(a)). These results are consistent with the results in Refs. [19, 20, 22]. The $A_p^{2/3}$ dependence in the forward hemisphere is expected in limiting fragmentation models[4], where the projectile is seen as a contracted disc by the target nucleus. Fig. 1(b) shows the dependence of $\langle n_s^F \rangle$ and N_{int}. The values of $\langle n_s^F \rangle$ increase with the number of interacting nucleons. This dependence can be described by a linear relation $\langle n_s^F \rangle = 0.59 + 1.24 N_{int}$, which supports the idea of considering the nucleus-nucleus collisions as a superposition of nucleon-nucleus collisions. It is observed that the values of the shower particles emitted in the backward hemisphere are nearly constant, within experimental error, for projectiles of mass number larger than or equal to seven. This means that the creation of shower particles in the backward hemisphere is nearly independent of the projectile mass number at nearly the same incident energy. The values of both $\langle N_g^F \rangle$ and $\langle N_g^B \rangle$ seem to be unaffected by the mass number of the incident projectile.

Table 1. The average multiplicities of shower and grey particles in the forward and backward hemispheres, and the average number of interacting nucleons $\langle N_{int} \rangle$.

reaction	$\langle n_s^F \rangle$	$\langle n_s^B \rangle$	$\langle N_g^F \rangle$	$\langle N_g^B \rangle$	$\langle N_{int} \rangle$	Ref.
p+Em	1.50 ± 0.01	0.114 ± 0.02			1.0	[17]
^{4}He+Em	4.04 ± 0.01	0.23 ± 0.01			2.42	[17]
^{6}Li+Em	5.30 ± 0.15	0.41 ± 0.01	2.08 ± 0.08	0.98 ± 0.05	3.56	[23]
^{7}Li+Em	4.96 ± 0.03	0.40 ± 0.01	3.68 ± 0.20	0.94 ± 0.04	3.92 ± 0.12	[24]
^{12}C+Em	7.11 ± 0.02	0.42 ± 0.01	4.52 ± 0.20	1.38 ± 0.07	5.28 ± 0.18	[17]
^{16}O+Em	10.03 ± 0.30	0.46 ± 0.02	3.58 ± 0.15	0.97 ± 0.04	6.35 ± 0.27	[30]
	9.84 ± 0.19	0.38 ± 0.02	4.47 ± 0.13	1.22 ± 0.04	7.65 ± 0.12	present work
^{22}Ne+Em	9.85 ± 0.04	0.45 ± 0.01	4.80 ± 0.20	1.42 ± 0.08	8.06 ± 0.13	[17]
	9.71 ± 0.23	0.40 ± 0.02				[21]
^{28}Si+Em	11.36 ± 0.09	0.44 ± 0.02	4.98 ± 0.18	1.42 ± 0.07	9.49 ± 0.27	[17]
	11.43 ± 0.35	0.35 ± 0.02				[21]
^{32}S+Em	14.58 ± 0.48	0.46 ± 0.03	3.17 ± 0.14	0.82 ± 0.05	14.68	[22]

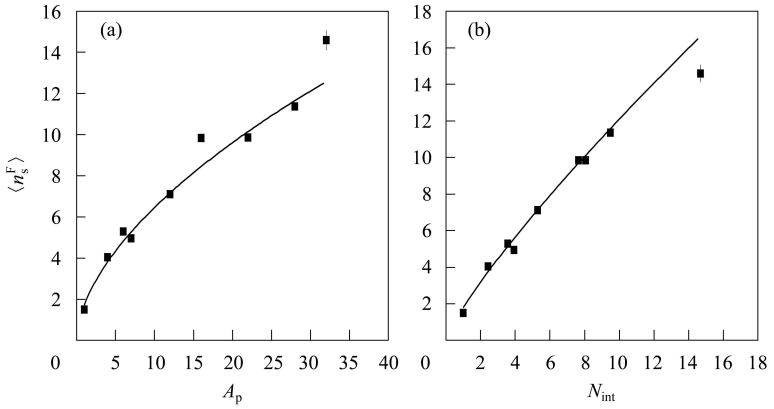

Fig. 1. The variation of $\langle n_s^F \rangle$ with A_p (a) and N_{int} (b).

The analysis of the experimental multiplicity distributions for the different emitted secondaries is one of the main sources of information on the mechanism of particle production. Therefore, a display of the multiplicity distributions for the shower and grey particles flying into forward and backward hemisphere in ^{16}O+Em interactions is performed. Fig. 2(a) shows the multiplicity distribution of the shower particles produced in the backward hemisphere, $p(n_s^B)$ for the interactions of ^{16}O with different emulsion target (i.e. CNO, Em, and AgBr) at 4.5 AGeV/c. It is very interesting to observe that all experimental data can be well reproduced by the exponential form:

$$p(n_s^B) = p_s e^{-\lambda_s^B n_s^B}, \quad (1)$$

which is consistent with the results of Abdelsalam[22]

for projectiles (^{12}C, ^{22}Ne, ^{28}Si and ^{32}S) with emulsion nuclei at the Dubna energy. This relation represents the fundamental equation of decay of an excited system, which emits pions in the backward hemisphere. The parameters λ_s^B and p_s, as obtained from the best fit of the experimental data, are listed in Table 2. For comparison the corresponding results from the interactions of ^{12}C, ^{22}Ne, ^{28}Si and ^{32}S with emulsion nuclei are also presented in the table. From this table it is interesting to observe the near constancy of the values of the decay constant λ_s^B for the interactions of all used projectiles with emulsion nuclei at 4.5 AGeV/c. Since the same target is used, these results also support the effective target model[4] where the incident nucleons are assumed to interact and excite in collective fashion with the row of nucleons along their paths. During de-excitation, pions are emitted in a manner similar to that in thermal models. This conclusion is also consistent with the model of Fredriksson[15], in which the incident nucleons interact collectively with all matter within 1 fm (in the rest frame) at the line of collision. It is obvious from Fig. 2(a) and Table 2 that the value of the decay constant, λ_s^B, decreases as target size increases for the same projectile.

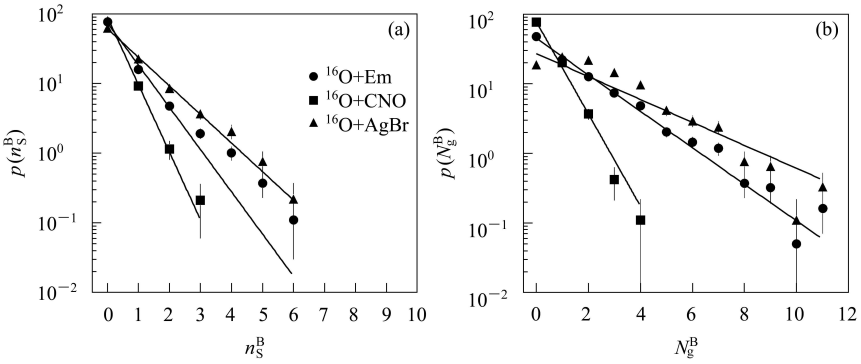

Fig. 2. The normalized multiplicity distribution of shower (a) and grey (b) particles emitted in the backward hemisphere of the interactions of ^{16}O with different emulsion targets together with linear fitting (straight lines).

Table 2. The fitting parameters of the backward shower and grey particle distributions fitted in a decay exponential law form.

projectile	target	λ_s^B	p_s	λ_g^B	p_g	Ref.
^{12}C	Em	1.09±0.04	63.22±7.75	0.75±0.06	45.92±11.56	[22]
^{16}O	CNO	2.23±0.09	89.19±3.05	1.52±0.05	77.53±2.72	this work
^{16}O	Em	1.40±0.04	74.01±2.01	0.60±0.02	44.76±1.33	this work
^{16}O	AgBr	0.94±0.04	60.91±2.44	0.38±0.01	27.04±1.12	this work
^{22}Ne	Em	1.06±0.04	58.52±6.98	0.66±0.04	40.91±7.58	[22]
^{28}Si	Em	1.02±0.08	54.93±13.14	0.67±0.04	42.11±8.88	[22]
^{32}S	CNO	2.38±0.10	86.86±11.22	1.81±0.04	83.07±6.64	[22]
^{32}S	Em	1.05±0.05	62.67±7.06	0.76±0.02	50.88±5.23	[22]
^{32}S	AgBr	0.89±0.05	61.68±6.97	0.67±0.03	52.77±7.68	[22]

Figure 2(b) shows the multiplicity distributions of the backward grey particles produced in the interactions of ^{16}O with different emulsion targets. The experimental data can be fitted by an equation similar to that describing the backward shower particles, i.e.

$$p(N_g^B) = p_g e^{-\lambda_g^B N_g^B}. \quad (2)$$

The fitting parameters λ_g^B and p_g are also listed in Table 2. For comparison the corresponding results from the interaction of ^{12}C, ^{22}Ne, ^{28}Si and ^{32}S with emulsion are also presented in Table 2. It is clearly seen that the values of λ_g^B are constant within experimental errors for interactions of different projectiles with the same target (Em). On the other hand, the values of λ_g^B decrease with increasing target mass for the same projectile.

The above results for shower and grey particles emitted in the backward hemisphere confirm the limiting fragmentation hypothesis at the incident momentum used. Therefore, the shower particles flying above the kinematic limit in the backward hemisphere

may be thought to be due to the decay of an exciting system at a fixed temperature in the first step. Then the backward grey particles will be emitted in the second step.

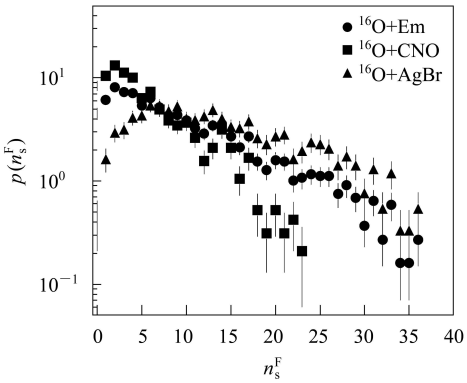

Fig. 3. The normalized multiplicity distribution of shower particles emitted in the forward hemisphere of the interactions of ^{16}O with different emulsion targets (CNO, Em and AgBr).

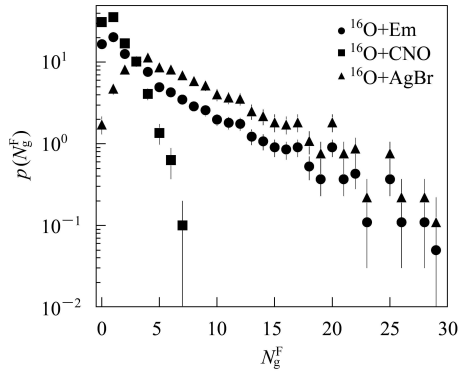

Fig. 4. The normalized multiplicity distribution of grey particles emitted in the forward hemisphere of the interactions of ^{16}O with different emulsion targets(CNO, Em and AgBr).

Figures 3 and 4 present the experimental multiplicity distributions of shower and grey particles in the forward hemisphere for the interactions of ^{16}O with different emulsion targets at 4.5 AGeV/c, respectively. The distributions are broader than those in the backward hemisphere (see Fig. 2(a) and (b)). This is due to the fact that in the forward hemisphere, there are contributions from both projectile and target participants while in the backward hemisphere the target size is the only affecting parameter. From these figures it also can be seen that the probability of producing such particles increases with increasing target size: the heavier the target, the broader the multiplicity distributions. This result is confirmed in Table 1 by the average numbers of shower and grey particles in both the backward and forward hemispheres.

The correlations between the multiplicities of the different types of particles emitted in the backward and forward hemisphere are one of the most sensitive sources of information on the mechanism of particle production in both the forward and backward hemispheres. Fig. 5 presents the relations between $\langle n_s^F(n_s^B)\rangle$ and n_s^B (a), $\langle n_s^B(n_s^F)\rangle$ and n_s^F (b) for ^{16}O+Em interactions at 4.5 AGeV/c respectively. The fitting of the experimental data of the figure gives the values of slopes b_F and b_B, from the following two relations:

$$\langle n_s^F\rangle = a_F + b_F n_s^B\,, \tag{3}$$

$$\langle n_s^B\rangle = a_B + b_B n_s^F\,. \tag{4}$$

The values of b_F and b_B are listed in Table 3. For comparison the corresponding results for ^{7}Li+Em, ^{22}Ne+Em and ^{28}Si+Em interactions at 3, 4.1 and 4.5 AGeV/c respectively are also presented in the table. From the analysis of Fig. 5 and Table 3, it may be noticed that a strong correlation between $\langle n_s^F\rangle$ and n_s^B, $\langle n_s^B\rangle$ and n_s^F can be seen. Also, from the table, one may notice that b_F increases with increasing projectile mass, which means that $\langle n_s^F\rangle$ increases with projectile mass number, while $\langle n_s^B\rangle$ remains nearly constant, within experimental error.

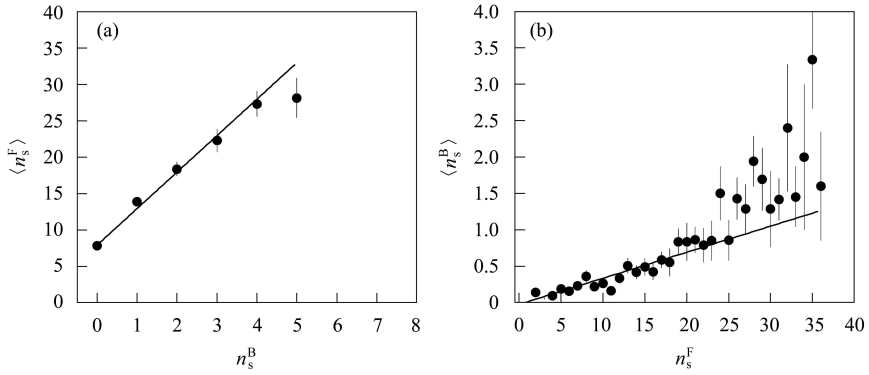

Fig. 5. The value of $\langle n_s^F\rangle$ as a function of n_s^B (a) and $\langle n_s^B\rangle$ as a function of n_s^F (b) for 4.5 AGeV/c ^{16}O+Em interactions.

Table 3. The values of slopes for ^{16}O+Em interactions at 4.5 AGeV/c and the corresponding results from Ref. [24].

projectile	target	$b_{\rm F}$	$b_{\rm B}$	Ref.
^{7}Li	Em	3.18 ± 0.15	0.032 ± 0.001	[24]
^{16}O	Em	5.01 ± 0.23	0.036 ± 0.002	this work
^{22}Ne	Em	6.43 ± 0.18	0.029 ± 0.002	[24]
^{28}Si	Em	8.14 ± 0.41	0.017 ± 0.002	[24]

Figure 6 shows the multiplicity correlations for various particles (shower, grey and black) in the forward and backward hemispheres as a function of $N_{\rm h}$ in the interactions of ^{16}O+Em at 4.5 AGeV/c. These correlations can be approximately fitted by a positive linear dependence with fitting parameters listed in Table 4. For comparison the results from ^{28}Si and ^{32}S+Em interactions are also presented in the table. From Fig. 6 and Table 4 we can conclude that the average multiplicity of shower particles emitted in the forward hemisphere strongly depends upon the number of heavily ionized particles $N_{\rm h}$, but the average multiplicity of backward shower particles weakly depends upon the number of $N_{\rm h}$, and this dependence increases with increasing projectile size at the same incident energy. The mean multiplicity of grey particles emitted in the backward hemisphere weakly depends upon the number of $N_{\rm h}$ and this dependence also increases with the increase of the projectile size at the same incident energy.

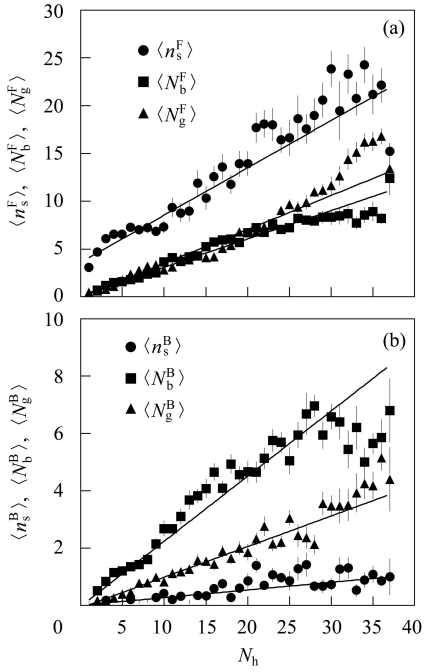

Fig. 6. The dependence of the average shower, grey and black particle multiplicities emitted in the forward (a) and backward (b) hemisphere for the ^{16}O+Em interaction on $N_{\rm h}$.

Table 4. The fitting parameters for the correlation of the average multiplicities of shower, grey and black particles emitted in the backward and forward hemispheres from different projectile induced emulsion interactions at 4.5 AGeV/c with $N_{\rm h}$.

correlation	^{16}O+Em		^{28}Si+Em[25]		^{32}S+Em[22]	
	slope	intercept	slope	intercept	slope	intercept
$\langle n_{\rm s}^{\rm F}\rangle$-$N_{\rm h}$	0.50 ± 0.01	3.59 ± 0.17	0.726 ± 0.012	2.383 ± 0.254	0.76 ± 0.03	5.64 ± 0.62
$\langle N_{\rm g}^{\rm F}\rangle$-$N_{\rm h}$	0.355 ± 0.005	-0.44 ± 0.03	0.290 ± 0.009	-0.018 ± 0.154	0.28 ± 0.02	-0.25 ± 0.44
$\langle N_b^{\rm F}\rangle$-$N_{\rm h}$	0.296 ± 0.004	0.13 ± 0.03			0.38 ± 0.02	-0.48 ± 0.38
$\langle n_{\rm s}^{\rm B}\rangle$-$N_{\rm h}$	0.027 ± 0.002	0.008 ± 0.013	0.034 ± 0.001	-0.010 ± 0.014	0.052 ± 0.004	-0.15 ± 0.07
$\langle N_{\rm g}^{\rm B}\rangle$-$N_{\rm h}$	0.107 ± 0.003	-0.082 ± 0.017	0.076 ± 0.002	-0.123 ± 0.052	0.084 ± 0.01	-0.17 ± 0.08
$\langle N_b^{\rm B}\rangle$-$N_{\rm h}$	0.227 ± 0.003	-0.033 ± 0.019			0.23 ± 0.01	0.35 ± 0.17

Figure 7 shows the multiplicity correlations for various particles emitted in the backward and forward hemispheres as a function of the number of interacting projectile nucleons $N_{\rm int}$ in the interactions of ^{16}O+Em at 4.5 AGeV/c. These correlations also can be fitted by a positive linear dependence with fitting parameters presented in Table 5. It can be concluded that the dependence of the average multiplicity of different particles emitted in the backward and forward hemispheres on $N_{\rm int}$ is the same as the correlation of the mean multiplicity of various backward and forward particles with $N_{\rm h}$.

Table 5. The fitting parameters for the correlation of the average multiplicities of shower, grey and black particles emitted in the backward and forward hemispheres from ^{16}O+Em interactions at 4.5 AGeV/c with $N_{\rm int}$.

correlation	slope	intercept
$\langle n_{\rm s}^{\rm F}\rangle$-$N_{\rm int}$	1.13 ± 0.02	0.89 ± 0.10
$\langle N_{\rm g}^{\rm F}\rangle$-$N_{\rm int}$	0.432 ± 0.015	0.703 ± 0.071
$\langle N_b^{\rm F}\rangle$-$N_{\rm int}$	0.288 ± 0.012	1.352 ± 0.083
$\langle n_{\rm s}^{\rm B}\rangle$-$N_{\rm int}$	0.043 ± 0.003	0.027 ± 0.015
$\langle N_{\rm g}^{\rm B}\rangle$-$N_{\rm int}$	0.127 ± 0.006	0.195 ± 0.033
$\langle N_b^{\rm B}\rangle$-$N_{\rm int}$	0.227 ± 0.010	0.913 ± 0.067

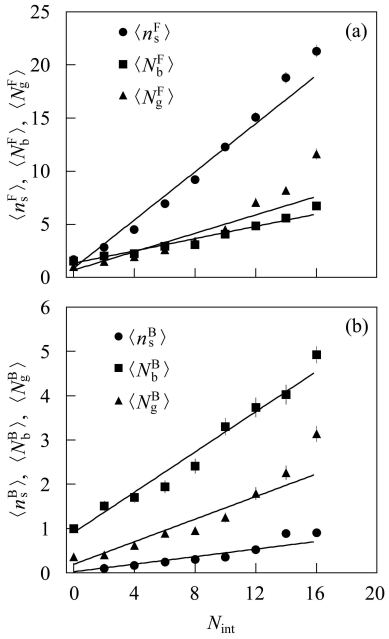

Fig. 7. The dependence of the average shower, grey and black particle multiplicities emitted in the forward (a) and backward (b) hemisphere for the ^{16}O+Em interaction on $N_{\rm int}$.

4 Conclusions

In studying the 4.5 AGeV/c ^{16}O+Em interaction, the following conclusions can be drawn.

1) The average multiplicity of shower particles emitted in the backward hemisphere remains nearly constant, with experimental error, for projectile mass number in larger than or equal to seven, but the average multiplicity of forward shower particles increases with increasing projectile size (or number of interacting projectile nucleons).

2) The correlation parameters for the shower particles emitted in the forward hemisphere increase with projectile mass number, whereas for the backward emission they decrease slightly as the projectile mass increases.

3) The average values of shower particles emitted in the forward and backward hemispheres increase linearly with the target fragments $N_{\rm h}$ or the number of interacting projectile nucleons.

4) The multiplicity distributions of the backward shower and grey particles are fitted by an exponential form with decay constant independent of the projectile size. However, a decrease in the values of decay constant is noted as the target size increases.

We are grateful to Professor I. Otterlund of the Lund University in Sweden for supplying the emulsion plates.

References

1 Frankfurt L L, Strikman M I. Phys. Lett. B, 1979, **83**: 497
2 Schroeder L S, Chessin S A, Geaga J V et al. Phys. Rev. Lett., 1997, **28**: 1787
3 Baldin A M et al. Sov. J. Nucl. Phys., 1976, **29**: 629
4 Mathis H B, MENG T C. Phys. Rev. C, 1978, **18**: 952
5 Burov V V, Lukyanov V K, Titov A I. Phys. Lett. B, 1977, **67**: 46
6 Yukawa T, Furui S. Phys. Rev. C, 1979, **20**: 2316
7 Fujita T, Hufner J. Nucl. Phys. A, 1979, **314**: 317
8 Geaga J V, Chessin S A, Grossiord J Y et al. Phys. Rev. Lett., 1980, **45**: 1993
9 Schmidt I A, Blankenbecler R. Phys. Rev. D, 1977, **15**: 3321
10 Gorenstein M I, Zinoviev G M. Phys. Lett. B, 1977, **67**: 100
11 Bubnov V I, Gaitinov A Sh, Eremenko L E et al. Z. Phys. A, 1981, **302**: 133
12 Fung S Y, Gore W, Kiernan G P et al. Phys. Rev. Lett., 1978, **41**: 1592
13 Hecman H H, Crawford H J, Greiner D E et al. Phys. Rev. C, 1978, **17**: 1651
14 Adamovich M I et al.(EMU01 Collaboration). Phys. Lett. B, 1990, **234**: 180; Phys. Rev. Lett., 1989, **62**: 262; Phys. Lett. B, 1990, **242**: 512
15 Fredriksson S. Phys. Rev. Lett., 1980, **45**: 1371
16 El-Nadi M, Ali-Mossa N, Abdelsalam A. Nuovo Cimento A, 1997, **110**: 1255
17 El-Nadi M, Abdelsalam A, Ali-Mossa N. Int. J. Mod. Phys. E, 1994, **3**: 811
18 El-Nadi M, Abdelsalam A, Ali-Mossa N. Radiat Phys. Chem., 1996, **47**: 681
19 El-Nadi M, Abdelsalam A, Ali-Mossa N et al. Eur. Phys. J. A, 1998, **3**: 183
20 El-Nadi M, El-Nagdy M S, Ali-Mossa N et al. Nuovo Cimento A, 1998, **111**: 1243
21 El-Naghy A, Sadek N M, Mohery M. Nuovo Cimento A, 1997, **110**: 125
22 Abdelsalam A, Shaat E A, Ali-Mossa N et al. J. Phys. G, 2002, **28**: 1375
23 Abdel-Waged K. J. Phys. G, 1999, **25**: 1721
24 Abd-Allah N N. Int. J. Mod. Phys. E, 2002, **11**: 105
25 Ahmad T, Irfan M. Phys. Rev. C, 1992, **46**: 1483
26 ZHANG D H. Chin. Phys., 2002, **11**: 1254
27 WU F J, ZHANG D H, LI J S et al. Chin. Phys., 2004, **13**: 646
28 LI J S, ZHANG D H, LI Z Y et al. Chin. Phys., 2004, **13**: 836
29 ZHANG D H, LI Z Y, LI J S et al. Chin. Phys., 2004, **13**: 1239
30 Abd-Elhalim S M, Callet A. Chaos, Solitons and Fractals, 2003, **18**: 115